Journal of Research in Pharmacy
Research Article
www.jrespharm.com

Manufacture, characterization and *in vitro* drug release studies of chitosan-PVA-MNPs hydrogel essenced drug delivery system for anticancer drug quercetin

Münteha ÖZSOY[1]*, Mahsa HEIDARNEJAD[2,3]

1 Department of Pharmaceutical Toxicology, Faculty of Pharmacy, Kocaeli Healthy and Technology University, Başiskele 41190, Kocaeli, Turkey.
2 Sakarya University, Biomaterials, Energy, Photocatalysis, Enzyme Technology, Nano and Advanced Materials, Additive Manufacturing, Environmental Applications and Sustainability Research and Development Group (BIOENAMS R&D Group), 54050 Sakarya, Turkey.
3 Department of Chemistry, Institute of Natural Sciences, Sakarya University, 54187, Sakarya, Turkey.
* Corresponding Author. E-mail: munteha.ozsoy@kocaelisaglik.edu.tr

Received: 24 September 2024 / Revised: 31 October 2024 / Accepted: 31 October 2024

ABSTRACT: In the current study, chitosan (CS) and polyvinyl alcohol (PVA) essenced hydrogels were produced using the freeze-thaw method without toxic cross-linking agents. Magnetic nanoparticles (MNPs) and quercetin (QC) were added to the system after synthesizing the hydrogel and the samples were freeze-dried using a lyophilizer. The prepared samples were used in in vitro drug release studies. QC, known as a natural polyphenol, is a promising candidate to support cancer treatment with its antioxidant effects. However, the hydrogels containing Fe3O4 nanoparticles exhibit high porosity and encapsulation efficiency, making them a convenient carrier for drug loading and controlled release. The QC was encapsulated in the synthesized CS-PVA-MNPs. Morphological changes of the prepared hydrogels were visualized using scanning electron microscopy (SEM). The molecular structure of the synthesized samples was determined using fourier transform infrared spectroscopy (FTIR), while their thermal stability was evaluated through thermogravimetric analysis (TGA). The encapsulation efficiency (EE) and drug loading efficiency (DLE) of QC in hydrogels including Fe_3O_4 MNPs were determined as 93.40% and 65.58%, respectively. In vitro release profiles of QC at pH 5 and pH 7.4 demonstrated the effectiveness of the hydrogel. These results indicate that CS-PVA-MNPs-QC is a convenient carrier for the intended drug delivery and reveal the potential of QC as a drug versus cancer cells.

KEYWORDS: Chitosan; polyvinyl alcohol; hydrogels; Fe_3O_4 MNPs; quercetin; drug delivery systems; drug release

1. INTRODUCTION

Cancer remains a substantial cause of death entire world; its prevalence is predicted to increase due to population growth and aging, especially in less developed regions where approximately 82% of the global population resides [1]. To increase comfort and alleviate side effects during the traditional cancer treatment process, antioxidant additives are used in addition to medications.

Natural polyphenols attract great attention in cosmetics, medicine, and food because of their well-rounded functions like antibacterial, antioxidant, and anticancer properties. Chemical groups in natural polyphenols (i.e. pyrogallol and catechol) are liable for strong non-covalent interactions through hydrophobic interactions and multiple hydrogen bonds, as well as dynamic covalent complexation with multiple metal ions and boronate groups. Natural polyphenols have been widely used in producing biomaterials like hydrogels, nanoparticles (NPs), and nanocapsules for transporting different types of molecules. Moreover, natural polyphenols comprised of umpteen pyrogallol/catechol groups can be readily combined with diverse polymers to evolve functional materials [2].

Chitosan is produced through the deacetylation of chitin; it is a natural biopolymer that is biocompatible, easily accessible, biodegradable, non-toxic and has an antimicrobial effect. CS is widely used in biomedical and medical applications like tissue engineering, drug delivery systems, and biosensors. Organic crosslinking agents used when preparing hydrogel with CS cause negative effects on the human body. Concerns remain regarding the safety of CS-essenced hydrogels, particularly due to the toxicity of glutaraldehyde. Possible side effects can be prevented by using a natural and non-toxic cross-linking agent

How to cite this article: Özsoy M, Heidarnejad M. Manufacture, characterization and in vitro drug release studies of chitosan-PVA-MNPs hydrogel essenced drug delivery system for anticancer drug quercetin. J Res Pharm. 2025; 29(1): 360-369.

https://dx.doi.org/10.29228/jrp.2022.00
ISSN: 2630-6344

or by boosting the freezing-thawing times [3]. In the literature, many drug carriers such as MNPs, hydrogels, and liposomes have been designed using chitosan and its derivatives [4,5].

Hydrogels are structures with three-dimensional polymeric networks. They have high water absorption capacities and can easily mimic cells. These materials do not irritate the body due to their flexibility and softness [8]. Bahareh et al. developed two biomolecules containing CMCS-grafted glycerol and CS-grafted glycerol hydrogels for controlled and sustained drug release. These hydrogels effectively delivered drugs to MCF-7 and other breast cancer cells with improved bioavailability [5].

NPs have been employed as drug carriers in implementations, also implicating cancer treatments, to utilize the therapeutic advantages of drug targets. With diameters ranging from 10 to 100 nm, nanoparticles exhibit distinctive and customizable physicochemical properties aimed at improving drug availability, targeting specificity to tissues, and enhancing drug solubility [6]. There are various drug delivery systems created by incorporating nanoparticles into hydrogels. Naderi et al. carried out drug loading and release studies for curcumin with the carboxymethyl CS hydrogel they synthesized by incorporating Fe_3O_4 and $MnFe_2O_4$ nanoparticles [7].

Quercetin is a flavonoid compound found in the composition of many foods such as onions, coriander, lovage, capers, berries, and apples. By stopping some key signal transduction targets, QC prevents cancer as well as healing tumor cells. However, other solvents, such as ethanol, are needed to be used during the studies due to the low solubility of QC in water. In recent studies, Patel et al. revealed that the in vivo cytotoxicity of QC-loaded polymer lipid hybrid NPs in breast cancer therapy was higher than free QC in terms of performance [8].

The current study explains the production of an extremely fruitful magnetic composite hydrogel for QC by incorporating CS-PVA-Fe_3O_4 MNPs as reinforcement. This study, it was aimed to synthesize a biocompatible hydrogel without using toxic and harmful cross-linkers, and the loading and in vitro release studies of QC, an adjuvant drug in cancer treatment, were carried out on the synthesized hydrogel to minimize the side influences of cancer treatment. The results obtained showed that hydrogel synthesis was successful through characterization studies and drug release through in vitro tests.

2. RESULTS

2.1 Characterization of Hydrogels

The manufacturing scheme CS-PVA-MNPs-QC hydrogel is shown in Figure 1. In light of studies in the literature, the hydroxyl and amine groups in chitosan both enable binding to Fe_3O_4 and play a role in polymerization by binding to PVA chains [9]. Thus, a cross-linked network-like hydrogel structure with porous and highly swelling properties in an aqueous environment is formed. Additionally, thanks to the magnetic property gained by the inclusion of Fe_3O_4 MNPs in the synthesized hydrogels, it provides the hydrogels with the advantage of being easily separated from the QC-released environment with an external magnetic field. Characterization studies of CS-PVA-MNPs-QC hydrogel were examined with various analytical techniques and explained below.

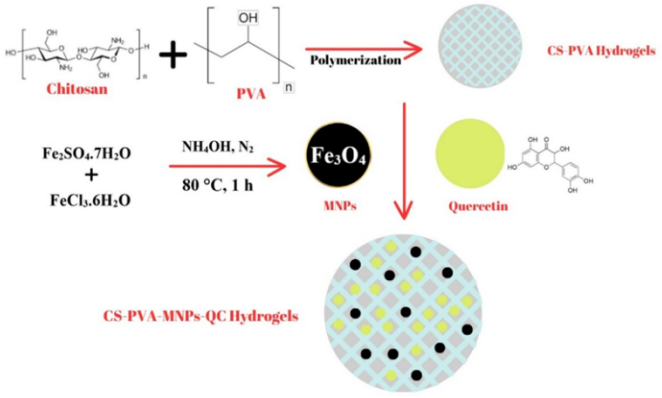

Figure 1. Schematic representation of the manufacturing of CS-PVA-MNPs-QC hydrogels

SEM images of all the prepared hydrogel samples are illustrated in Figure 2. The CS-PVA hydrogel surfaces exhibit a high degree of porosity, which is associated with the freezing process. CS contributes to an

increase in the porosity of the hydrogel structure and results in wider pores [4]. The three-dimensional network seen in the SEM images (Figure 2 A, B, C) can be attributed to the presence of crystalline regions formed by PVA chains. The conformational alterations in PVA, which provides binding capabilities within the hydrogel, are caused by the freeze-thaw cycle. Moreover, the porosity and pore structure arise from a freezing process dependent on the solvent, which leads to the formation of ice crystals that expand until they meet the surfaces of other crystals. During the freeze-drying of the hydrogels, these ice crystals undergo sublimation, leaving behind channels formed by gaps. In Figure 2B, MNPs are visible within these gaps as white dots. Structural transformations that occurred when QC was integrated into the hydrogel are visible in Figure 2C.

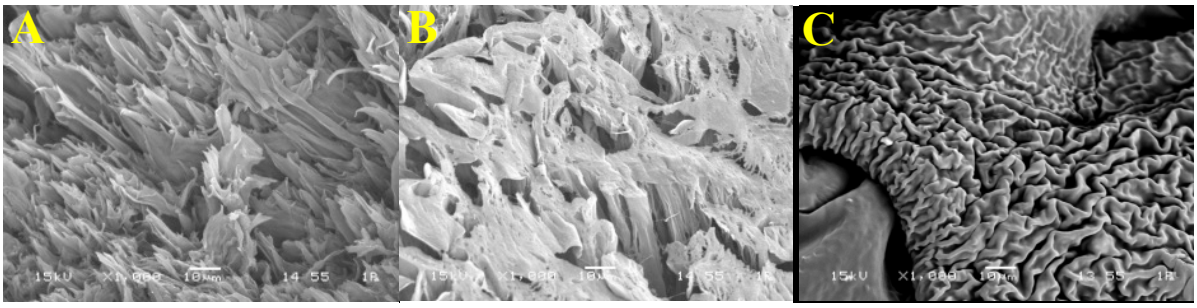

Figure 2. SEM images of (A) CS-PVA, (B) CS-PVA-MNPs, and (C) CS-PVA-MNPs-QC hydrogels.

For a better understanding of magnetic behavior, the response of synthesized Fe_3O_4 MNPs to an external magnet in a dispersion environment is presented in Figure 3. In future studies, the magnetic properties of MNPs can be utilized for targeted drug delivery.

Figure 3. Presentation of confirming that Fe_3O_4 MNPs are attracted towards the external magnet

The FTIR spectrum of chitosan is shown in Figure 4. A significant peak at 3353 cm^{-1}, which can be linked to –OH stretching vibrations. The absorption bands at 1650 cm^{-1} (C=O) and 1550 cm^{-1} (–NH–) correspond to amide groups [10]. A decline in the absorbance between 1145 and 1000 cm^{-1} is attributed to the vibration bands of the –C–O–C– groups, indicating the molecular splitting of chitosan chains [11]. n pure PVA, distinct peaks were noted such as the broad band at 3290 cm^{-1} related to the O-H stretching vibrations. The 1619 cm^{-1} peak corresponds to the C=C stretching of PVA, while the 1161 cm^{-1} peak is related to C–O bond stretching, and the 1015 cm^{-1} peak is associated with C–O–C bond stretching [12]. An intense peak at 590 cm^{-1} represents Fe-O bond stretching in Fe_3O_4, confirming the presence of Fe_3O_4 MNPs [13]. Key peaks such as 3326 cm^{-1} (N-H and O-H stretching), 2825 cm^{-1} and 2856 cm^{-1} (C-H stretching), 1545 cm^{-1} (C=O stretching), 1508 cm^{-1} (N–H bending), 1378 cm^{-1} (C–O stretching), 1213 cm^{-1} (N-C-N stretching), 1071 cm^{-1} (C-O-C stretching), and 590 cm^{-1} (Fe-O stretching) indicate the successful integration of MNPs into the hydrogel. The CS-PVA-MNPs spectrum further confirms this with the presence of Fe-O vibrations at 590 cm^{-1} and various other key peaks. The FTIR spectrum of quercetin (QC) displays several key peaks: C=C

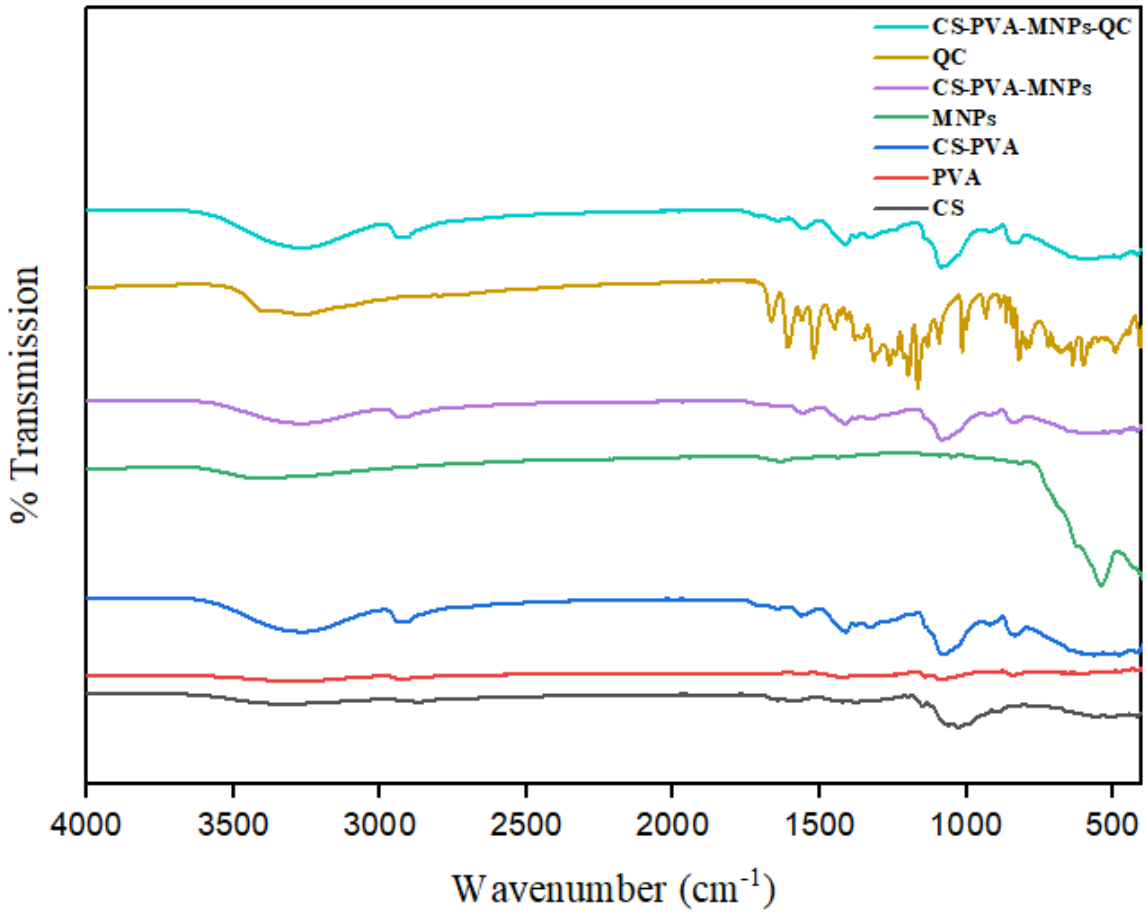

Figure 4. FTIR spectra for manufactured drug delivery system

stretching at 1659 and 1636 cm^{-1}, aromatic C=C stretching and C-H in-plane deformation at 1605 and 1587 cm^{-1}, along with aromatic C=C and C=O stretching at 1558 and 1563 cm^{-1}. Additional stretching vibrations of C=C and C=O, accompanied by C-H in-plane deformation, are observed at 1511 cm^{-1}, 1504 cm^{-1}, 1462 cm^{-1}, and 1454 cm^{-1}. Peaks at 1424 cm^{-1} and 1419 cm^{-1} are linked to O-H and C-H in-plane deformation, and further vibrations at 1350 cm^{-1} and 1372 cm^{-1} correspond to aromatic C=C and C=O stretching. The peaks at 1311 and 1308 cm^{-1} suggest aromatic C=O stretching, while additional aromatic C=O and O-H in-plane deformations appear between 1286 cm^{-1} and 1265 cm^{-1}, as well as between 1240 cm^{-1} and 1248 cm^{-1}. The range between 1198 cm^{-1} and 1191 cm^{-1} captures aromatic C=C and O-H deformations. Peaks in the 1091–1093 cm^{-1} range relate to C=C and C=O stretching, while peaks between 1014 cm^{-1} and 1022 cm^{-1} suggest C=O stretching. Peaks at 997–1000 cm^{-1} correspond to O-H in-plane deformation, while aromatic C=O stretching occurs between 930 cm^{-1} and 936 cm^{-1}. C-H out-of-plane deformation is observed at 881 and 872 cm^{-1}, alongside additional peaks at 841 and 840 cm^{-1}, which also show C-H out-of-plane deformation and aromatic C=O stretching. The peaks at 807 cm^{-1} and 817 cm^{-1} represent further out-of-plane deformations, with torsional vibrations at 785 and 783 cm^{-1} [14]. The intensity of these peaks, particularly the aromatic C-O stretches, remains relatively unchanged with QC loading, as observed in the CS-PVA-MNPs hydrogel. However, the peak at 1600 cm^{-1} increases slightly due to the overlapping of C=O stretching bands from QC and PVA. Additionally, interactions between QC and the hydroxyl groups of Fe_3O_4 NPs slightly enhance the peak at 3500 cm^{-1} [15,16]. All findings obtained from the FTIR spectra proved that every step of the synthesis occurred correctly.

As shown in Figure 5 TGA can indicate the formation of a coating on the surface of magnetite nanoparticles [17]. In the given study, Initial Mass Loss (0-200 °C), in this range is likely due to the evaporation of moisture or solvents [18]. Major Decomposition (200-400 °C), significant mass loss phase corresponds to the decomposition of the polymer matrix (CS-PVA) and possibly the organic components in the sample. Final Mass Loss (400-600 °C): Further decomposition of the remaining material, which could include the degradation of chitosan and any other organic additives. The slight variations between the curves of CS-PVA, CS-PVA-MNPs, and CS-PVA-MNPs-QC indicate that the addition of magnetic

nanoparticles and quercetin slightly alters the thermal stability and decomposition profile of the base CS-PVA material [19-21].

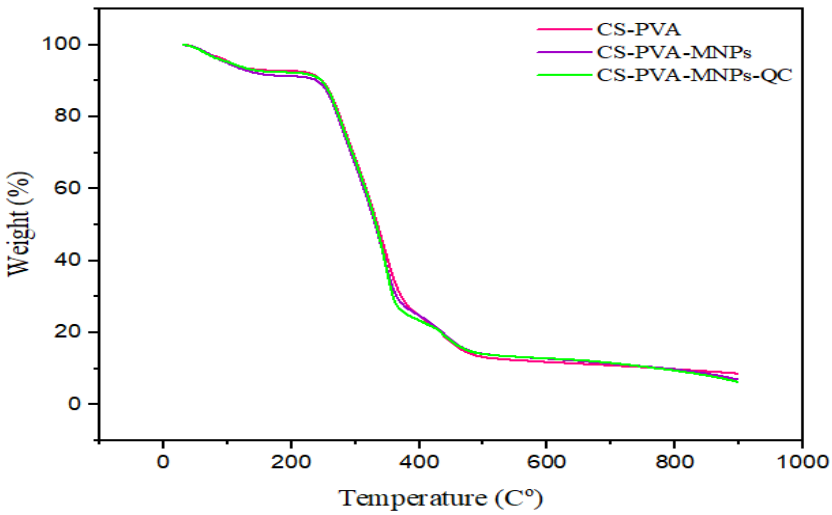

Figure 5. TGA curves CS-PVA, CS-PVA-MNPs and CS-PVA-MNPs-QC

2.2 Assays of Swelling

The changes in the hydrogel's weight during soaking in water at room temperature for 96 hours are illustrated in Figure 6. The increase in weight during the swelling test, followed by a subsequent decrease, is related to the hydrogel's water absorption capacity and the release of water from the hydrogel matrix, respectively [22]. The initial rapid swelling observed in the first few hours is due to the hydrogel's rapid water absorption. During this period, the hydrogel matrix quickly absorbs water, leading to an increase in weight. As water absorption continues, the hydrogel matrix reaches saturation, and the rate of water absorption decreases [23]. The weight continues to increase during the first three hours as the hydrogel matrix continues to absorb water, though at a slower rate. Following this, partial release or expulsion of water from the hydrogel begins, leading to a decrease in the hydrogel's weight. The decrease in weight after 96 hours indicates that the hydrogel's water absorption capacity has largely reached saturation, and it has started to release some of the absorbed water [24]. This process illustrates the water absorption and release capabilities of the hydrogel, which is essential for characterizing hydrogel materials.

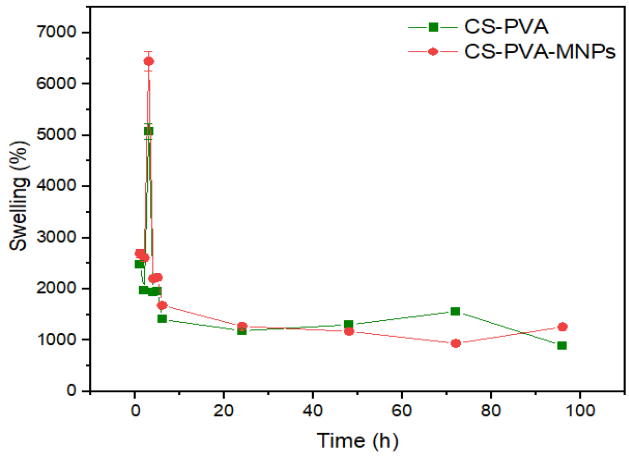

Figure 6. Swelling kinetics of CS-PVA and CS-PVA-MNPs hydrogels

2.3 Loading Capacity and Encapsulation Efficacy of Quercetin

For the determination of DLC and EE, the absorbance and calibration curve of the QC solution was used as a reference, and the DLC and EE results were obtained by UV measurements at 370 nm. QC loading capacity and encapsulation efficiency were determined as 65.58% and 93.4%, respectively shown in Figure 7. For CS-PVA-MNPs-QC hydrogel. In a drug loading study conducted in the literature for QC, Eshaghi et al. reached 48% DLC and 89% EE for the TiO2-containing PVP/PVA hydrogels they synthesized [16]. In another study, Ahmadi et al. reached 42%, 57% DLCs and 72%, 94% EEs for the CS-MMTQC and Fe2O3-CS-MMTQC they synthesized, respectively [8]. The DLC and EE of the developed CS-PVA-MNPs-QC hydrogel in this study are compatible with the literature and are quite high. This can be explained by the drug retention effect of MNPs in addition to the increase in the porosity of chitosan in the structure.

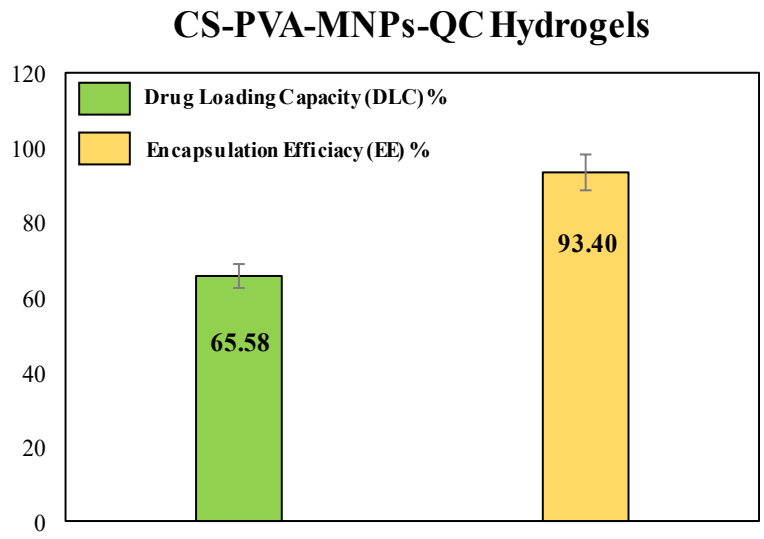

Figure 7. DLC and EE for QC loading to the CS-PVA-MNPs-QC hydrogel

2.4 Evaluation of *In Vitro* Drug Release Properties of Synthesized Hydrogel

As depicted in Figure 8, the burst QC release for CS-PVA-MNPs-QC is 69.9% at pH 5.0 in the first 6 h. Again, at the same pH, 24 and 48 hour releases are 78.77% and 85.45%, respectively. For CS-PVA-MNPs-QC, the releases for 6, 24, and 48 hours at pH 7.4 are 22.07%, 38.79% and 42.49%, respectively. At the end of 96 hours, 98.2% of QC was released from the hydrogel at pH 5, while this rate was 43.77% at pH 7.4. In an acidic medium (pH 5.0), the CS' amino groups protonate and positively charge, thus increasing the hydrophilicity and intramolecular electrostatic repulsions, resulting in dramatic swelling of the CS-PVA hydrogel. With the protonation of the CS amino groups, Schiff base bonds become unstable and dissociation of QC occurs [3]. According to the in vitro release profile, it is observed that hydrogel is much faster to release QC at pH 5.0 than at pH 7.4. Consequently, a pH-sensitive controlled release process for acid-triggered burst release can be achieved.

3. DISCUSSION

CS-PVA hydrogels were successfully developed by integrating MNPs as drug carriers for QC. The analysis results were characterized using SEM and FTIR, while the synthesis procedures for CS-PVA-MNPs-QC hydrogels were validated independently. The attraction of Fe3O4 MNPs to an external magnetic field is a key aspect for enhancing magnetic-targeted drug delivery in future research. The swelling test results further confirmed the hydrogel's capacity for water absorption and release. The fluctuations in hydrogel weight during the swelling test directly correlate with its water-holding ability and subsequent release of water from the matrix. The QC loading capacity and encapsulation efficiency of the CS-PVA-MNPs-QC

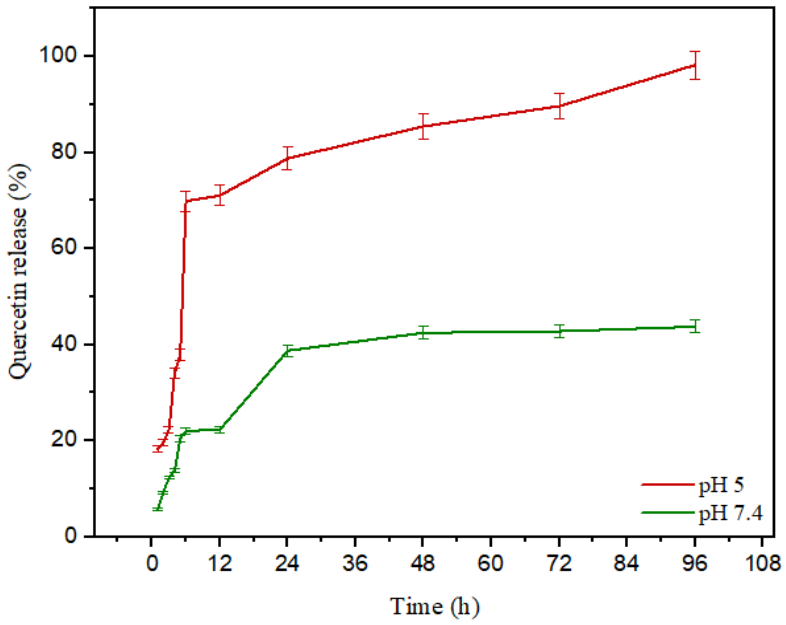

Figure 8. In vitro QC release from CS-PVA-MNPs-QC hydrogel at pH 5.0 and pH 7.4. Results are acquired as mean ± SD (n = 3).

hydrogel were observed to be significantly high, measured at 65.58% and 93.4%, respectively. Due to the beneficial effects of phenolic compounds in cancer therapy, the high QC efficiency provides a strong advantage for continued research. According to in vitro drug release tests on the CS-PVA-MNPs-QC hydrogel in both acidic (pH 5.0) and physiological (pH 7.4) environments, the release of QC was consistently higher at pH 5 compared to pH 7.4, with measurements taken at hourly intervals. At pH 5, QC release rates were 78.77%, 85.45%, and 98.2% after 24, 48, and 96 hours, respectively, whereas at pH 7.4, the rates were significantly lower at 38.79%, 42.49%, and 43.77% over the same periods. These results confirm the successful creation of the intended drug delivery system and its effectiveness in vitro. The therapeutic potential and efficacy of this system warrant further investigation.

4. CONCLUSION

In this study, a novel chitosan-PVA hydrogel incorporating MNPs was successfully synthesized and characterized as a drug delivery system for quercetin. The hydrogel demonstrated favorable properties, including enhanced biocompatibility, stability, and a high drug-loading capacity. Through in vitro drug release studies, it was observed that the release of quercetin was both pH-dependent and sustained over time, which is ideal for targeting cancer cells in acidic environments. The incorporation of MNPs also offers the potential for magnetically guided drug delivery, enhancing therapeutic precision. Overall, the developed hydrogel system holds promise for improving the efficacy of anticancer treatments while minimizing side effects.

5. MATERIALS AND METHODS

5.1 CS-PVA Hydrogel Synthesis

Considering the ratios in the literature for CS-PVA hydrogel synthesis, 400 mg CS was admixed with 0.1 M acetic acid solution as 2% (w/w) for 1 night at room temperature (RT). It was prepared by mixing 2000 mg PVA and 10% solution at 80 °C for 1 hour. Then two solutions were admixed with ratio (1:1, v/v) until homogeneous at RT. The mixture was placed in a petri dish and degassed for 1 hour at atmospheric pressure [4,25].

5.2 MNPs Synthesis

Fe_3O_4 synthesis was carried out with the mole ratio Fe^{2+}: Fe^{3+} = 1: 1.75, considering the literature-mentioned ratios [26]. 2 g $Fe_2SO_4.7H_2O$ and 3.4030 g $FeCl_3.6H_2O$ were supplemented to 300 mL distilled

water and stirred under N_2 atmosphere at 80 °C. 40 mL ammonia solution (25%) was added drop by drop into the solution and stirred for 1 hour. To remove excess base in the mixture after synthesis, washing was carried out once with hot distilled water and twice with normal distilled water, and the MNPs were dried at 70 °C overnight after collecting with a magnet.

5.3 CS-PVA@MNPs Synthesis

15 mg MNPs were added onto the prepared chitosan-PVA with a (w:w) ratio of Fe_3O_4: CS-PVA (1: 16.67) and mixed until homogeneous distribution was achieved [27]. The mixture was placed in a petri dish and degassed for 1 hour at atmospheric pressure [4,25].

5.4 CS-PVA@MNPs@Quercetin Synthesis

400 µL of quercetin at a concentration of 1 mg/mL was prepared and added dropwise to 20 mL of Chitosan-PVA-MNPs solution, resulting in a final drug concentration of 20 µg/mL in the solution [8]. The mixture was placed in a petri dish and degassed for 1 hour at atmospheric pressure [4,25]. CS-PVA-MNPs and CS-PVA-MNPs-QC hydrogels were subjected to vacuum freeze-drying to prepare them for drug release processes and characterization tests. First, the freezing and thawing cycle was repeated six times in the freezer to achieve the desired gel consistency. It was then dried in the Biobas Lyophilizer device for 48 hours, making it ready for use, and stored in the refrigerator for further characterization.

5.5 Assays of Swelling

The water absorption capacity and swelling behavior of CS-PVA and CS-PVA-MNPs hydrogels in deionized water at RT were analyzed gravimetrically for 96 hours. After weighing the dry weight of the lyophilized hydrogel pieces in air were transferred to Falcon® tubes containing 50 mL of deionized water and shaken at RT. After being immersed for certain periods, the hydrogel pieces were taken from the swelling environment, excess water was removed, weighed, and the measurements were recorded [4]. The degree of swelling of the hydrogel at certain times was calculated using Equation (1):

$$\mathrm{SD}\ (\%) = \left[\left(\frac{Ws - Wd}{\mathrm{Wd}}\right)\right] \times 100 \quad (1)$$

where ws and wd are the wet weight and the dry weight of the hydrogel, respectively.

The swelling reached equilibrium at 24 h, and then the swelling equilibrium state, q, was calculated via Equation (2):

$$q = \frac{Ws}{\mathrm{Wd}} \quad (2)$$

5.6 Drug Loading Study for Quercetin

Using ultraviolet-visible spectrophotometry (UV), the DLC and EE of QC were calculated as shown in equations (3) and (4).

$$\text{Drug loading capacity}\ (\%) = \frac{\text{Amount of drug in carrier (mg)}}{\text{Amount of carrier (mg)}} \times 100 \quad (3)$$

$$\text{Drug loading capacity}\ (\%) = \frac{\text{Amount of drug in carrier (mg)}}{\text{Amount of carrier (mg)}} \times 100 \quad (4)$$

5.7 *In Vitro* Quercetin Release Studies from Hydrogels

To elucidate the drug release properties of the developed CS-PVA-MNPs-QC, in vitro drug release tests were achieved in an acidic medium (pH 5.0, 37 °C) and physiological medium (pH 7.4, 37 °C). For the drug release test, CS-PVA-MNPs-QC samples of 1 mg.mL-1 were spread separately into 15 mL of pH 5.0 and pH 7.4 buffers and then sealed in dialysis bags. Dialysis bags were immersed one by one in 50 mL of buffer solutions (pH 5.0 and pH 7.4) and mixed with a magnetic stirrer at 37°C and 100 rpm for 72 hours. At predetermined times, 1 mL of release medium was separated and refreshed with fresh buffer solutions each time to maintain ambient conditions. The drug amounts in the samples taken from the release media were determined UV spectrophotometrically at 370 nm. The released drug percentage was calculated via Equation (5).

$$Drug\ release\ (\%) = \frac{Amount\ of\ drug\ release\ time\ 't'}{Amount\ of\ drug\ release\ at\ time = 0} \times 100 \quad (5)$$

Acknowledgements: M.O. thanks to the Kocaeli Health and Technology University and Sakarya University for their partial support.

Author contributions: Münteha Özsoy, a significant contribution to concept and design, a significant contribution to data collection, and methodology, drafted the article and critically reviewed the manuscript for important intellectual content. Mahsa Heidarnejad significant contribution to data collection, significant contribution to analysis, and interpretation of data.

Conflict of interest statement: The authors of this study declare that they have no conflict of interest.

REFERENCES

[1] Torre LA, Bray F, Siegel RL, Ferlay J, Lortet-Tieulent J, Jemal A. Global cancer statistics, 2012. CA Cancer J Clin. 2015; 65(2): 87–108. https://doi.org/10.3322/caac.21262 PMID: 25651787

[2] Özsoy M. PhD Thesis. Synthesis, characterization, and investigation of anticancer effects of polyphenol-doped ZIF-8 metal organic cage drug carrier systems. Department of Biochemistry, Faculty of Chemistry, Sakarya University, Sakarya, Turkey, 2023.

[3] Rahimi S, Khoee S, Ghandi M. Preparation and characterization of rod-like chitosan–quinoline nanoparticles as pH-responsive nanocarriers for quercetin delivery. Int J Biol Macromol. 2019; 1(128): 279–289. https://doi.org/10.1016/j.ijbiomac.2019.01.137

[4] Figueroa-Pizano MD, Vélaz I, Peñas FJ, Zavala-Rivera P, Rosas-Durazo AJ, Maldonado-Arce AD. Effect of freeze-thawing conditions for preparation of chitosan-poly (vinyl alcohol) hydrogels and drug release studies. Carbohydr Polym. 2018; 1(195): 476–485. https://doi.org/10.1016/j.carbpol.2018.05.004

[5] Wang Y, Wang Z, Lu W, Hu Y. Review on chitosan-based antibacterial hydrogels: Preparation, mechanisms, and applications. Int J Biol Macromol. 2024; 255: 128080. https://doi.org/10.1016/j.ijbiomac.2023.128080

[6] Xiao B, Adjei-Sowah E, Benoit DSW. Integrating osteoimmunology and nanoparticle-based drug delivery systems for enhanced fracture healing. Nanomed: Nanotechnol Biol Med. 2024; 56: 102727. https://doi.org/10.1016/j.nano.2023.102727

[7] Naderi Z, Azizian J. Synthesis and characterization of carboxymethyl chitosan/Fe3O4 and MnFe2O4 nanocomposites hydrogels for loading and release of curcumin. J Photochem Photobiol B: Biol. 2018; 185: 206–214. https://doi.org/10.1016/j.jphotobiol.2018.06.014

[8] Ahmadi M, Pourmadadi M, Ghorbanian SA, Yazdian F, Rashedi H. Ultra pH-sensitive nanocarrier based on Fe2O3/chitosan/montmorillonite for quercetin delivery. Int J Biol Macromol. 2021; 30(191): 738–745. https://doi.org/10.1016/j.ijbiomac.2021.09.023 PMID: 34517028

[9] Viney C, Case ST. International Journal of Biological Macromolecules: Editorial statement. Int J Biol Macromol. 1999; 26(1): 1–2. https://doi.org/10.1016/S0141-8130(99)00101-4

[10] Farasati Far B, Omrani M, Naimi Jamal MR, Javanshir S. Multi-responsive chitosan-based hydrogels for controlled release of vincristine. Commun Chem. 2023; 6(1): 1–14. https://doi.org/10.1038/s42004-023-00829-1

[11] Pawlak A, Mucha M. Thermogravimetric and FTIR studies of chitosan blends. Thermochim Acta. 2003; 396(1): 153–166. https://doi.org/https://doi.org/10.1016/S0040-6031(02)00523-3

[12] Enoch K, S RC, Somasundaram AA. Improved mechanical properties of Chitosan/PVA hydrogel – A detailed rheological study. Surf Interface. 2023; 1: 41. https://doi.org/10.1016/j.surfin.2023.103178

[13] Kim DH, Nikles DE, Brazel CS. Synthesis and characterization of multifunctional chitosan-Mnfe2o4 nanoparticles for magnetic hyperthermia and drug delivery. Materials (Basel). 2010; 3(7): 4051–4065. https://doi.org/10.3390/ma3074051

[14] Çakar S, Özacar M. The effect of iron complexes of quercetin on dye-sensitized solar cell efficiency. J Photochem Photobiol A Chem. 2017; 346: 512–522. https://doi.org/10.1016/j.jphotochem.2017.07.006
[15] Catauro M, Papale F, Bollino F, Piccolella S, Marciano S, Nocera P. Silica/quercetin sol–gel hybrids as antioxidant dental implant materials. Sci Technol Adv Mater. 2015; 1: 16. https://doi.org/10.1088/1468-6996/16/3/035001
[16] Eshaghi MM, Pourmadadi M, Rahdar A, Díez-Pascual AM. Improving quercetin anticancer activity through a novel polyvinylpyrrolidone/polyvinyl alcohol/TiO2 nanocomposite. J Drug Deliv Sci Technol. 2023; 1: 81. https://doi.org/10.1016/j.jddst.2023.104304
[17] Zhao SY, Don KL, Chang WK, Hyun GC, Young HK, Young SK. Synthesis of magnetic nanoparticles of Fe3O4 and CoFe2O4 and their surface modification by surfactant adsorption. Bull Korean Chem Soc. 2006; 27(2): 237–242. https://doi.org/10.5012/bkcs.2006.27.2.237
[18] Enev V, Sedláček P, Jarábková S, Velcer T, Pekař M. ATR-FTIR spectroscopy and thermogravimetry characterization of water in polyelectrolyte-surfactant hydrogels. Colloid Surf A Physicochem Eng Asp. 2019; 575: 1–9. https://doi.org/10.1016/j.colsurfa.2019.04.089
[19] Rusu AG, Popa MI, Lisa G, Vereştiuc L. Thermal behavior of hydrophobically modified hydrogels using TGA/FTIR/MS analysis technique. Thermochim Acta. 2015; 613(1): 28–40. https://doi.org/10.1016/j.tca.2015.05.018
[20] Enev V, Sedláček P, Řihák M, Kalina M, Pekař M. IR-Supported thermogravimetric analysis of water in hydrogels. Front Mater. 2022; 9: 1–8. https://doi.org/10.3389/fmats.2022.931303
[21] Huang Y, Lu J, Xiao C. Thermal and mechanical properties of cationic guar gum/poly(acrylic acid) hydrogel membranes. Polym Degrad Stab. 2007; 92(6): 1072–1081. https://doi.org/10.1016/j.polymdegradstab.2007.02.011
[22] Wang T, Gunasekaran S. State of water in chitosan–PVA hydrogel. J Appl Polym Sci. 2006; 101(5): 3227–3232. https://doi.org/https://doi.org/10.1002/app.23526
[23] Agnihotri S, Mukherji S, Mukherji S. Antimicrobial chitosan–PVA hydrogel as a nanoreactor and immobilizing matrix for silver nanoparticles. Appl Nanosci. 2012; 2(3): 179–188. https://doi.org/10.1007/s13204-012-0080-1
[24] Fan L, Yang H, Yang J, Peng M, Hu J. Preparation and characterization of chitosan/gelatin/PVA hydrogel for wound dressings. Carbohydr Polym. 2016; 146: 427–434. https://doi.org/10.1016/j.carbpol.2016.03.002
[25] Figueroa-Pizano MD, Vélaz I, Martínez-Barbosa ME. A freeze-thawing method to prepare chitosan-poly (Vinyl alcohol) hydrogels without crosslinking agents and diflunisal release studies. J Vis Exp. 2020; 1: 155. https://doi.org/10.3791/59636
[26] Atacan K, Özacar M. Characterization and immobilization of trypsin on tannic acid modified Fe3O4 nanoparticles. Colloid Surf B Biointerface. 2015; 128: 227–236. https://doi.org/https://doi.org/10.1016/j.colsurfb.2015.01.038
[27] Hingrajiya RD, Patel MP. Fe3O4 modified chitosan based co-polymeric magnetic composite hydrogel: Synthesis, characterization and evaluation for the removal of methylene blue from aqueous solutions. Int J Biol Macromol. 2023; 31: 244. https://doi.org/10.1016/j.ijbiomac.2023.125251